Trans Indian Inst Met
https://doi.org/10.1007/s12666-019-01658-4

TECHNICAL PAPER

Design and Development of Dielectric Resonator Antenna Using Ceramic Materials: An Overview

Shukdev Pandey[1] · Devendra Kumar[1] · Om Parkash[1] · Lakshman Pandey[2]

Received: 30 August 2018 / Accepted: 14 March 2019

Abstract The basics of design of microstrip aperture-coupled ceramic rectangular dielectric resonator antenna (RDRA) are given. Methods of estimation of antenna dimensions, impedance matching, excitation procedure and choice of suitable materials to be used in the fabrication are briefly described. The RDRA dimensions are obtained by solving the transcendental equation derived from Maxwell equations using dielectric waveguide model. Some ceramics are found useful for fabrication of DRAs that yield large bandwidth and gain are summarized. An attempt to explore the application of dielectric materials having small dielectric loss (tan $\delta > 0.01$) has been made by developing RDRA configurations using one, two and three element arrays, and effect of dielectric loss on their performance is studied using ANSYS HFSS simulations. For a RDRA array comprising of three elements, where the middle parasitic element has small dielectric loss (tan $\delta \sim 0.1$) and the outer elements are aperture coupled, the gain decreases only by 2.7%, while the bandwidth is enhanced by 3%. The findings indicate the possibility of using ceramics having small dielectric loss such as $Ba_{1-x}Sr_xTiO_3$ ($x = 0.35$, tan $\delta \sim 0.1$) with some trade-off with gain by using suitable designs. Equivalent circuit modelling useful in understanding the performance of microstrip aperture-coupled RDRA is also presented.

✉ Lakshman Pandey
pandeyl@hotmail.com

[1] Department of Ceramic Engineering, IIT(BHU), Varanasi 221005, India

[2] Department of Post Graduate Studies and Research in Physics and Electronics, Rani Durgavati University, Jabalpur 482001, India

Keywords Ceramics · Dielectric resonator antenna · RDRA · Equivalent circuit

1 Introduction

An antenna is defined as that part of a transmitting or receiving system which is designed to radiate or to receive electromagnetic waves in an efficient and desired way. An antenna is usually connected to a transmission line and works as a transformer of voltage/current to electric/magnetic fields or vice versa. How to best make this connection, to design the antenna and to choose the material for fabrication of the antenna so that the signal being fed to the antenna is radiated in space in an efficient and desired way, is a very challenging subject. This becomes much more so since the performance of a well-designed isolated antenna may be quite different than when it is installed in the actual system such as a mobile handset [1–3].

The traditional antennas suffer from narrow bandwidth and reduced radiation efficiency due to increased losses at higher frequencies. This has lead to intensive efforts for better designs as well as for search of materials that may be used for fabrication of antenna [4, 5]. In the last two and a half decades, a new kind of antenna research has gained momentum, known as dielectric resonator antenna (DRA). It was conceived as early as in 1939 by Richtmyer [6], but the practical feasibility appeared after the work of Long et al. in 1983 [7] where it was shown that the dielectric resonators, well known from microwave circuits, can in fact become very efficient antennas if properly excited.

For successful development of DRA, two-pronged approach is useful. In one, workable geometrical designs are looked for taking into consideration the available materials. In the other, the material of which the resonator

Published online: 29 March 2019

is to be fabricated is looked at. By using same design, an antenna can be used at different frequencies by changing the material or vice versa [5, 8, 9].

Dielectric materials with suitable characteristics namely high relative permittivity, low loss tangent (tan $\delta \leq 0.01$) and very low temperature coefficient of resonance frequency (commonly termed as τ_f) are of utmost importance for developing DRAs. Search for such materials together with refined antenna designs constitutes a very hot topic at present [4, 5, 8]. Materials having small dielectric loss (tan $\delta > 0.01$) are considered not so useful for antennas. However, Zivkovich [10] has recently reported enhancement in bandwidth of wire antenna by loading it with a material having small dielectric loss (tan $\delta \sim 0.05$). Therefore, it is considered worthwhile to make an attempt to explore design of RDRA with a view to enhance the bandwidth by using ceramics with small dielectric loss (tan $\delta > 0.01$). In this paper, design of RDRA array involving one, two and three elements is presented and their performance is studied with different values of dielectric loss. The design is based on 35% Sr-doped $BaTiO_3$ ceramic synthesized and studied by us. General ideas regarding design of DRA are presented in Sect. 2.1. Few ceramics recently studied and found useful for development of DRA are briefly presented in Sect. 2.2. Design of RDRA array and study of performance are described in Sect. 2.3 where idea of equivalent circuit modelling is also given. Conclusions are given in Sect. 3.

2 Design and Development of RDRA

2.1 General Ideas

The main dimension of a DRA is proportional to the wavelength in the dielectric medium, $\lambda_0/\sqrt{(\mu_r\,\varepsilon_r)}$, where λ_0 is the free-space wavelength at the resonant frequency, μ_r and ε_r are relative permeability and relative permittivity, respectively [11, 12]. For a dielectric material, $\mu_r \approx 1$ and the dimension is reduced to $\lambda_0/\sqrt{\varepsilon_r}$. By using a dielectric with higher value of ε_r, DRA's can be miniaturized. The efficiency of an antenna depends upon inter-segment matching being satisfied in the design. The antenna is exposed to air (free space) on one side (radiating side) and connected to a signal source (of typical 50 Ω impedance) on some other rear side through a matched transmission line [12, 13]. However, there is a mismatch on the air side. The intrinsic impedance, η, of the antenna dielectric will be equal to $\eta_0\sqrt{(\mu_r/\varepsilon_r)}$ where η_0 is the intrinsic impedance of free space. A dielectric having numerically equal values of μ_r and ε_r will make η equal to η_0, and the antenna will be automatically impedance matched to free space and will help in achieving higher efficiency. Considerable efforts are being put to develop materials, especially ceramics, having high relative permittivity [14–18] and also where ε_r and μ_r can be tailored or varied by application of external fields. These are the so-called magneto-dielectric materials and have been the focus of intensive research activity recently [9, 19–24].

DRA's of various shapes such as spherical, hemispherical, cylindrical, rectangular have been reported. Out of all these shapes, the rectangular dielectric resonator antenna (RDRA) offers maximum flexibility of design as the dimensions (length a, width b and height d) can be suitably varied. [5, 8, 11, 25–27]. The basics of RDRA design are summarized now. Design of DRA essentially involves estimation of its dimensions for given resonance frequency, relative permittivity of the material and the modes to be excited. The modes (the patterns of electric and magnetic fields, **E** and **H**) that can exist in a DRA are obtained by using the so-called dielectric waveguide model (DWM) which treats a DRA as waveguide having its cross section same as the DRA (say $a \times b$), filled with the dielectric and truncated in the direction of propagation by a length (say d). It has been shown that rectangular DRA's support the so-called non-confined modes for which the boundary condition $\mathbf{E}.\mathbf{n} = 0$ is to be satisfied at all the surfaces of the resonator, where **E** denotes the electric field intensity and **n** denotes the normal to the surface of the resonator [8, 28].

The basic equations of electromagnetism (the Maxwell equations) are solved using these boundary conditions and expressions for field components are derived. The dominant mode is TE^{Z}_{111} where the superscript indicates the direction of propagation and the subscripts indicate the number of half wavelengths in the x, y and z directions. It has also been shown that lowest order non-confined modes radiate like magnetic dipoles [28]. The Maxwell equations can be solved analytically only for some well-defined waveguide shapes such as cylindrical and rectangular assuming that losses are negligible [12, 13]. For other situations, numerical methods are adopted. Computer programs involving various algorithms, such as ANSYS High-Frequency Structure Simulator (HFSS) software utilizing finite element method, have been developed which are readily available and are being widely used. By utilizing these softwares, the study of the performance of antennas of any desired designs has become possible by using simulation.

By solving Maxwell equations using DWM for a RDRA, relations for the field components H_z and E_z are given as

$$H_z = \frac{k_x^2 + k_y^2}{j\omega\mu_0} A \cos(k_x x) \cos(k_y y) \cos(k_z z) \quad (1)$$

$$E_z = 0 \quad (2)$$

where k_x, k_y and k_z denote the wave numbers along x, y and z directions, respectively, and A is an arbitrary constant [28]. The field components H_x, H_y, E_x and E_y are derived from H_z [12, 13, 28].

The values of k_x and k_y for the dominant TE^z_{111} mode are given as

$$k_x = \frac{\pi}{a} \tag{3}$$

$$k_y = \frac{\pi}{b} \tag{4}$$

The wave numbers k_x, k_y and k_z satisfy the equations

$$k_x^2 + k_y^2 + k_z^2 = \varepsilon_r k_0^2 \tag{5}$$

and

$$k_z \tan\left(\frac{k_z d}{2}\right) = k_{z0} \tag{6}$$

where

$$k_{z0} = \sqrt{\left[(\varepsilon_r - 1)k_0^2 - k_z^2\right]} \tag{7}$$

and k_0 is the wave number in free space. Equation (6) is also known as transcendental equation and arises from the continuity condition of the fields at the surface of the RDRA normal to the direction of propagation.

Using Eq. (6), d can also be expressed as

$$d = \frac{2}{k_z}\tan^{-1}\left(\frac{k_{z0}}{k_z}\right) \tag{8}$$

For TE^z_{111}, mode values of a, b and d lie between $\lambda/2$ and λ and $d < b < a$, λ being the wavelength in the guide [26, 29].

The resonator parameters can be computed in the following way. For a given value of relative dielectric permittivity, the wavelength in the material of the RDRA is calculated by using $\lambda = \lambda_0/\sqrt{\varepsilon_r}$ where λ_0 is the free-space wavelength for frequency f_0. The values of a and b are chosen so that $\lambda/2 < a < \lambda$, $\lambda/2 < b < a$ and $\lambda/2 < d < b$ (to have only TE_{111} modes). For given resonator dimensions a and b, dielectric constant ε_r and resonance frequency f_0, the values of k_x and k_y are first obtained from Eqs. (3) and (4). These are used to get the value of k_z from Eq. (5) which is then used in Eqs. (6) or (8) to calculate the value of d. In actual practice, the RDRA is usually placed on a large ground plane to avoid back radiations. Then, by making use of image theory, the dimension along the normal to the ground plane is made equal to half of that for the isolated RDRA [28].

Several feeding techniques exist for coupling of the RDRA to a microwave power source. These are named as probe feeding, microwave strip transmission line feeding, coplanar waveguide feeding and slot feeding [5]. The feed ends are so located and oriented near the DRA's that the emanating field lines enforce the field patterns of the desired modes in the DRA. Due to design simplicity and better coupling, the slot feeding, also known as aperture coupling, is very popular and involves a slot in the ground plane. The guided wave propagating along the microstrip transmission line is coupled, through the slot (aperture), to the resonant modes of the dielectric resonator. In this, the RDRA is centrally placed on a large ground plane supported by a substrate (e.g. FR4, dielectric constant 4.4, thickness (h) = 1.6 mm) having a printed microstrip line on the other side and usually extending up to the middle of the bottom of the RDRA or a little beyond. The ground plane also possesses an etched aperture of certain length and width oriented at right angles to the microstrip beneath the RDRA. For matching the microstrip line to a 50 Ω microwave power source, the width of the line can be estimated by using the relations given in Eqs. (9–11) for calculating its characteristic impedance Z_0 [12]. The line width, its length extending beyond the aperture, size of the aperture, dimensions of the DRA, etc., are optimized to achieve desired performance by using simulation softwares such as HFSS.

2.2 Some Ceramic Systems for DRA

A dielectric resonator antenna system involves a piece of dielectric material acting as a resonator placed on a ground plane supported by a substrate with some arrangement for coupling with the microwave signal source. The performance of the system is closely related to properties of the materials used for resonator and substrate. Vast literature on materials for microwave applications is available. Ceramics useful for microwave applications have been listed in detail by Sebastian et al. [30–33].

Due to increasing demand of large bandwidths and need to shift to higher frequency bands, there is a constant search for new low cost and easily preparable materials. Together with this, ease of manufacture of the whole system in compact integrated form is looked for. This requires sintering of the whole assembly containing all the components including the electrodes, such as silver and gold, at a suitable temperature and atmosphere to avoid degradation of electrodes. Depending upon the applications and ceramic materials, this cofiring is done in various temperature regions. This has given rise to the so-called high-temperature cofired ceramics (HTCC, sintering temperature > 950 °C), low-temperature cofired ceramics (LTCC, sintering temperature 700–950 °C) and ultra-low-temperature cofired ceramics (ULTCC, sintering temperature < 700 °C). LTCC usually contains glass, which lowers the firing temperature compatible with silver and gold. In the following sections, some ceramics recently used for DRA are briefly described.

$La(Mg_{0.5}Ti_{0.5})O_3$ ceramics have suitable microwave dielectric properties for the application of dielectric resonators, antenna and filters [34, 35]. However, their sintering temperatures are high (1500–1600 °C). By using B_2O_3–La_2O_3–MgO glass, Lin et al. [36] prepared $La(Mg_{0.5}Ti_{0.5})O_3$ ceramics which could be sintered at 850 °C and has excellent microwave dielectric properties ($\varepsilon_r = 11.8$, $Q \times f = 14{,}700$ and $\tau_f = 7.4$ ppm °C). This LTCC material has been prepared and used to fabricate dual-segment CDRA having a large bandwidth ($\sim$ 1.7 GHz) at resonance frequency of 6.31 GHz [37].

Low-firing bismuth-based ceramic is a kind of typical high-frequency dielectric with high relative permittivity and low dielectric loss and attracts more and more attention with the advancement in microelectronic technologies and microwave communication. Bismuth-based low-firing ceramics Bi_{3x} Zn_{2-3x-y} Ay $(Zn_x$ Nb_{2-x-z} $B_z)$ O_7 ($A = Ca^{2+}$, $B = Sb^{5+}$, Ti^{4+}, $x = 0.5$–0.67, $y = 0.2$–0.3, $z = 0.2$–1.4) with the dielectric constants of 97, 71 and 33, respectively, were synthesized by the conventional solid-state reaction method, and probe-fed DRA's of cylindrical and rectangular shapes were designed and fabricated to resonate at 2–4 GHz [38]. For study of the performance of RDRA in vicinity of human body and also to estimate the rate of electromagnetic energy absorption, known as specific absorption rate (SAR) in the body tissues, a RDRA was fabricated by using ($CaO{\cdot}4ZnO{\cdot}Nb_2O_5{\cdot}TiO_2$) ceramic material ($\varepsilon_r = 15.19$ and tan $\delta = 0.0192$) to operate at C-band of microwave frequencies (4–6 GHz) [39].

It has been found that DRAs show very low coupling compared to equally sized surface coils and can be used in transceiver arrays without requiring decoupling networks in magnetic resonance imaging (MRI). For patients comfort, DRA's of small sizes are needed. This can be achieved by using ceramics having high value of relative permittivity. Lead Zirconate Titanate (PZT) ceramic ($\varepsilon_r = 1070$) has been used to fabricate rectangular DRA's for magnetic resonance imaging (MRI) [40].

Ceramics called the lead zinc titanate ($Zn_{0.8}$ $Pb_{0.2}$ TiO_3, ZPT) have been used for fabrication of a probe-fed cylindrical DRA having gain of 3.68 and bandwidth of 3.34 GHz (i.e. 72.92%). This ceramic has $\varepsilon_r = 16$ and loss tangent = 0.01 which are independent of frequency in the range of 8–12.5 GHz [41]. Study of cylindrical DRA by using zirconium tin titanate ($Zr_{0.8}$ $Sn_{0.2}$) TiO_4 ceramic material (ZST) and resonating at 4.8 GHz has been carried out [42]. The sintering temperature for $(Zr_{0.8}$ $Sn_{0.2})TiO_4$ can be lowered from 1400 to 1200 °C by doping it with La_2O_3 and ZnO.

By using Li_2O–$1.94MgO$–$0.02Al_2O_3$–P_2O_5 (LMAP) ceramic ($\varepsilon_r = 6.2$, tan $\delta = 0.0006$) and Teflon ($\varepsilon_r = 2.1$, tan $\delta = 0.001$), a DRA, comprising coaxial probe-fed four-element composite triangular sections, was designed and fabricated. With a gain of 4.66 dB at the operating frequency of $\sim$ 11 GHz, a bandwidth of 7.6 GHz and monopole-like radiation patterns was obtained [43]. Ceramic (Zn, Mg)TiO_3 has been found to be good material for antenna. Addition of V_2O_5 significantly improves the densification and addition of glass additives in $(Zn_{1-x}$-$Mg_x)TiO_3$ (ZMT) lowers the sintering temperature. Ceramic systems $(Zn_{1-x}Mg_x)TiO_3$ (ZMT) were prepared with different substitutions of Mg in place of Zn ($x = 0.1$, 0.2, 0.3, 0.4) which have been used for development of CDRA. The values of relative permittivity and loss tangent lie in the ranges of (17–26) and (4.3–12.5) $\times$ 10^{-4}, respectively [44].

Barium strontium titanate ($Ba_{1-x}Sr_xTiO_3$) has been found to be a very suitable material for antenna fabrication. Barium strontium titanate added with PbO–BaO–B_2O_3–SiO_2 (10 wt%) glass has been used for fabrication of stacked RDRA. By adding the glass, the ceramic can be sintered at 800 °C. The relative dielectric permittivity is $\sim$ 27. This material has been used to develop two-segment filleted RDRA having bandwidth of $\sim$ 47.8% in the operating frequency range of 7.71–12.56 GHz [45].

$Ba_{1-x}Sr_xTiO_3$ ($x = 0.35$) prepared in our laboratory has $\varepsilon_r = 40$ with tan $\delta \sim 0.1$ at 10 GHz. As mentioned in Sect. 1, an attempt has been made to develop antenna designs to explore the possibility of application of such small loss ceramics in RDRA which is described in the next section.

2.3 Design of RDRA

The design essentially involves the estimation of the dimensions of the resonator for given values of relative dielectric permittivity (ε_r) and resonance frequency (f_0). The calculations were made for $Ba_{1-x}Sr_xTiO_3$ ($x = 0.35$) having $\varepsilon_r = 40$ at $f_0 = 10$ GHz.

The value of the wavelength, λ, in the dielectric is given as

$$\lambda = \frac{2\pi}{\sqrt{\omega^2 \mu_r \varepsilon_r}} = \frac{c}{f\sqrt{\varepsilon_r}} \frac{3 \times 10^8}{3 \times 10^9 \sqrt{40}} \; m = 4.74 \text{ mm}$$

We assume that dimension along x is 'a', along y is 'b', along z is 'd'.

For dominant TE^z_{111} mode, values of a and b were chosen such that $\lambda/2 < a < \lambda$, $\lambda/2 < b < \lambda$ and $b < a$. Here, $\lambda/2 = 2.37$ mm. Therefore, tentative values for a and b were chosen as $a = 4.5$ mm and $b = 3.5$ mm. Now, with the given values $f_0 = 10$ GHz, $a = 4.5$ mm, $b = 3.5$ mm, $\varepsilon_r = 40$, value of 'd' was calculated by using Eqs. (3)–(8) iteratively. A small computer program was written for this purpose. The program resulted in 'd' = 3.02 mm. So, we got the values as $a = 4.5$ mm,

b = 3.5 mm, d = 3.02 mm for ε_r = 40 and f_0 = 10 GHz. Number of combinations of a, b and d are possible that satisfy the above requirements.

Now, design of feed line has been described. A microstrip line on a FR4 (relative permittivity = 4.4, thickness = 1.6 mm) substrate was chosen for coupling the RDRA to a 50 Ω source. The corresponding width of the strip was estimated by using relations given by Eqs. (9)–(11) [12]

$$Z_0 = \frac{60}{\sqrt{\varepsilon_{\text{eff}}}} \ln\left(\frac{8h}{w} + \frac{w}{4h}\right), \quad \frac{w}{h} \leq 1 \tag{9}$$

$$Z_0 = \frac{1}{\sqrt{\varepsilon_{\text{eff}}}} \frac{120\pi}{\left[\frac{w}{h} + 1.393 + 0.667 \ln\left(\frac{w}{h} + 1.444\right)\right]}, \quad \frac{w}{h} \geq 1 \tag{10}$$

where w is the width of microstrip line placed on a substrate of relative dielectric permittivity ε_s and height h. ε_{eff} is the effective relative dielectric permittivity given by

$$\varepsilon_{\text{eff}} = \frac{(\varepsilon_s + 1)}{2} + \frac{(\varepsilon_s - 1)}{2\sqrt{1 + 12h/w}} \tag{11}$$

The desired width comes out to be 3.08 mm. A ground plane of dimensions 45 mm × 45 mm was chosen on the other side of which the strip resides. An aperture/slot of length L_s and width W_s located at the centre of the ground plane was used for aperture coupling. One RDRA element was centrally placed on the aperture. The microstrip was extended beyond the aperture to facilitate stub tuning. The parameters were optimized to give maximum bandwidth at resonance frequency of 10 GHz. A single RDRA is schematically shown in Fig. 1 (where $L = a$, $W = b$ and $H = d/2$). The reflection coefficient and gain obtained by HFSS for the same are shown in Fig. 2. The dimensions and other details are given in Table 1.

Now, design of an RDRA array comprising of three elements is described. For designing the array, two more similar RDRAs, apertures and microstrip lines were made which were placed on each side of the middle RRDA. These strips were joined together and further connected to the 50 Ω source through a matched line. The design of the array is schematically shown in Fig. 3a. The three 50 Ω microstrip lines give an impedance of 16.67 Ω at the joint. In order to match this with the 50 Ω source, a quarter wavelength section having impedance of $\sqrt{(50*16.67)}$ Ω was designed which was achieved by using a wider strip (15 mm) as shown in Fig. 3a. Figure 3b shows variation of reflection coefficient with frequency, and Fig. 3c shows gain for aperture-coupled array of three RDRAs with middle element parasitic. A RDRA array comprising of two RDRA elements was also designed, but for brevity the details are not given here.

The performance of the RDRA array configurations using one, two and three elements was studied by using

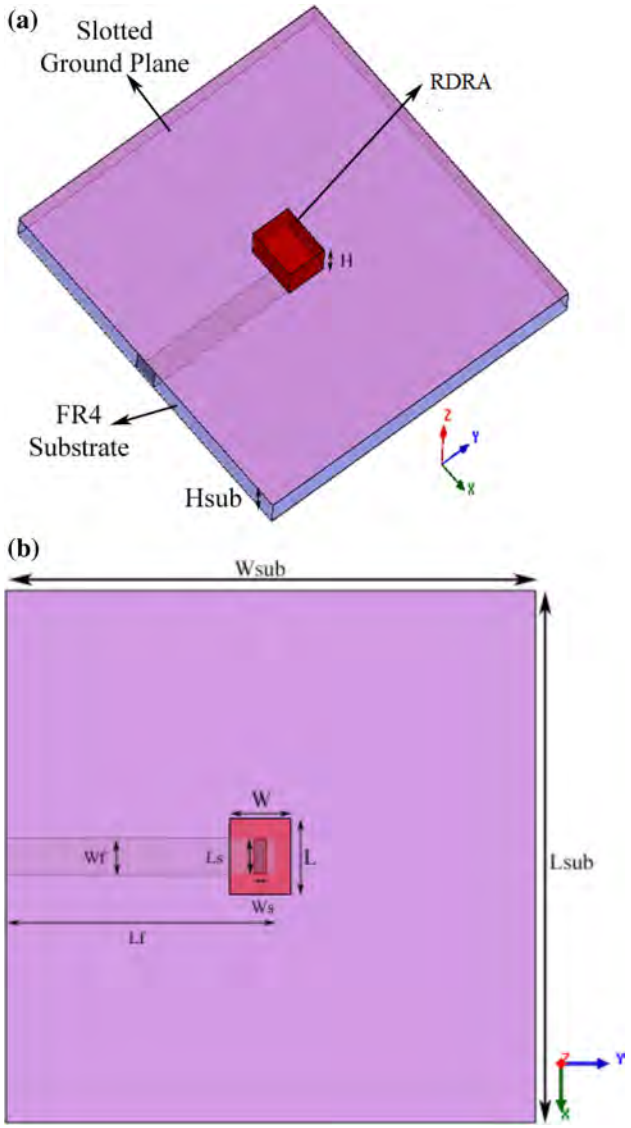

Fig. 1 Schematic diagram of aperture-coupled RDRA **a** 3-D view and **b** top view

ANSYS HFSS simulation software. Effect of increasing the value of dielectric loss in the elements on bandwidth, gain and shape of the far field pattern was observed. The results are summarized in Table 2. It is seen that for case (1) (a single RDRA), the bandwidth remains same but the gain and shape deteriorate when the dielectric loss is increased from 0.001 to 0.1. For case (2) (array of two RDRA elements), the bandwidth remains almost same but gain and shape deteriorate when the dielectric loss is increased from 0.001 to 0.1. For case (3) (RDRA array comprising of three elements), it is seen that when all the elements are aperture coupled and loss tangent increases from 0 to 0.1; in all the three elements, the bandwidth slightly increases, the gain decreases heavily by 62% and the shape of the far field pattern also deteriorates. For case (4) (RDRA array

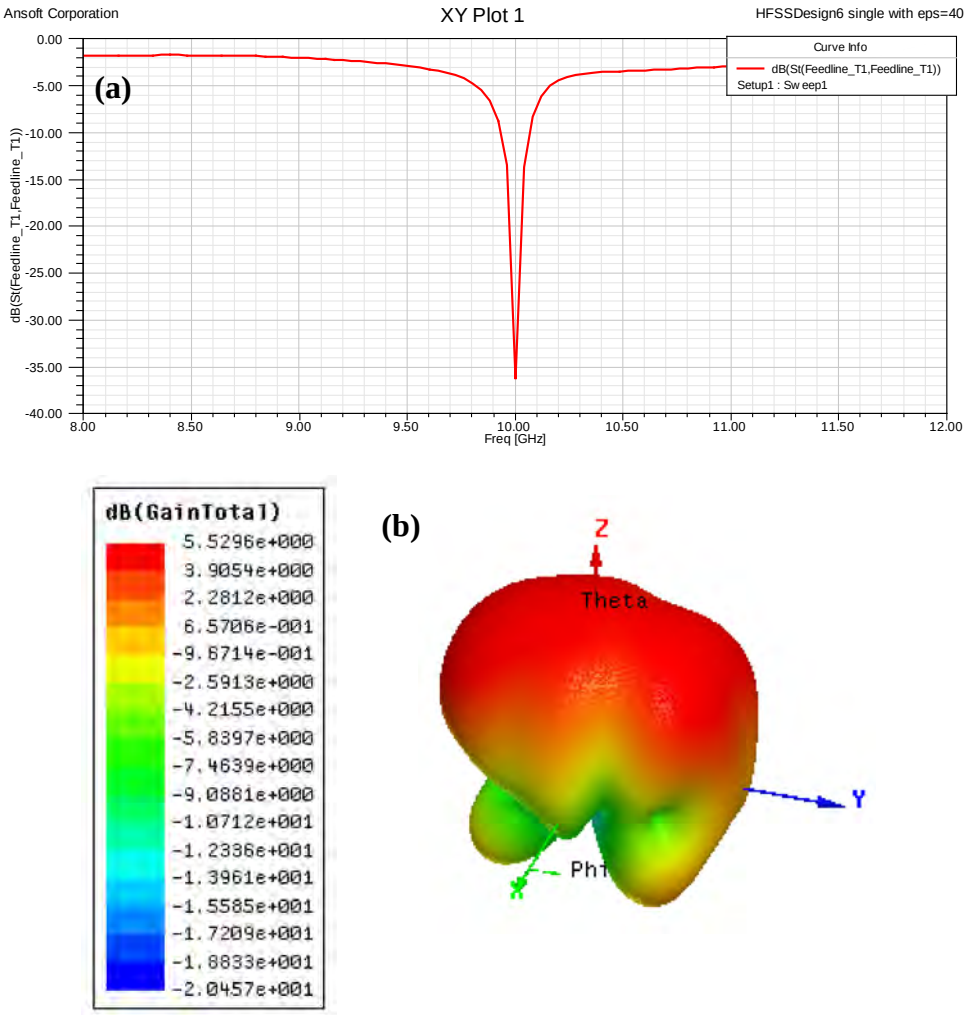

Fig. 2 **a** Variation of reflection coefficient with frequency and **b** gain for single RDRA

Table 1 Optimized values of parameters for the proposed antenna comprising of substrate of length L_{sub} and width W_{sub} with height H_{sub}, RDRA of length $L(= a)$ and width $W(= b)$ with height $H(= d/2)$, microstrip feed line of length L_f, width W_f, aperture/slot of length L_s and width W_s, the input impedance being 50 Ω

Parameter	W_{sub}	L_{sub}	H_{sub}	W	L	H	W_s	L_s	W_f	L_f
Size (mm)	45	45	1.6	4.5	3.5	1.5	1	1.9	1	23

comprising of three elements), it is found that when the outer elements are aperture coupled and the middle parasitic element is mutually coupled to the neighbouring elements, the band width slightly increases from 1.32 to 1.36 GHz as the dielectric loss in the middle element is increased from 0 to 0.1. The gain decreases from 5.97 to 5.81 dB (i.e. deteriorates only by 2.7%). Also, in this case, the far field pattern remains almost same as dielectric loss is increased. The results of case (4) indicate that ceramics such as $Ba_{1-x}Sr_xTiO_3$ having small loss ($\delta \sim 0.1$) can also be used for development of RDRA using suitable designs.

It has been reported by Huitema and Monediere [11] that for cylindrical DRA (CDRA), the impedance bandwidth is maximum when ε_r is around 10 and increases as the dielectric losses increase and is widest for $\varepsilon_r = 10$, whatever the losses. For a given ε_r, the radiation efficiency also decreases as the dielectric loss increases. However, for low relative dielectric permittivity (below about 40), even in case of a high loss material, the radiation efficiency remains higher than 50%. Thus, for wide bandwidth applications, ceramics with low ε_r, such as alumina ($\varepsilon_r \sim 10$) may be useful, whereas for miniature DRA, high ε_r ceramic is needed [11]. High relative permittivity and low

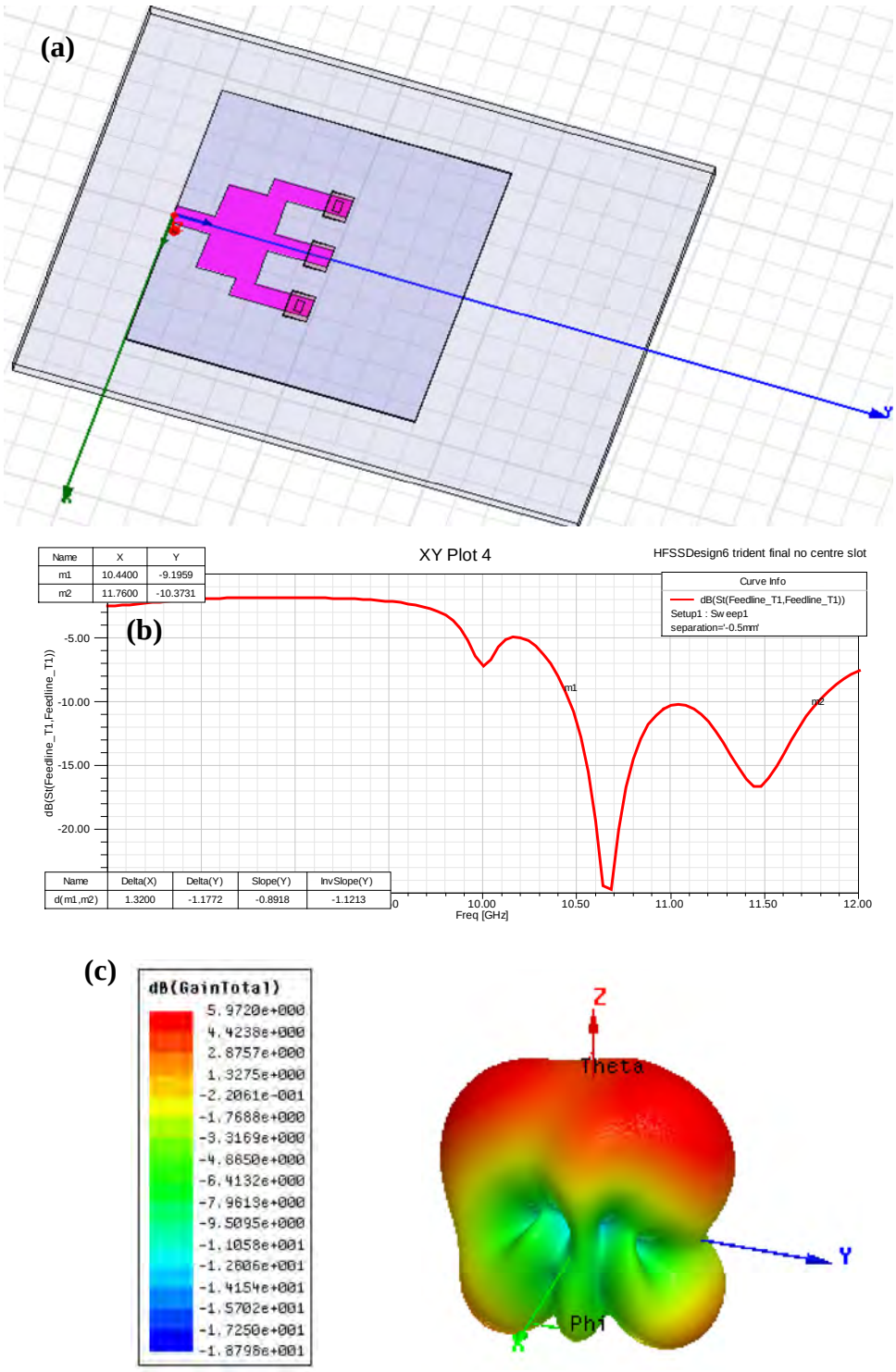

Fig. 3 **a** Design, **b** variation of reflection coefficient with frequency and **c** gain for aperture-coupled array of three RDRAs with middle element parasitic

loss materials are suitable for antenna fabrication, whereas those with small loss may be used for loading of antennas to get an enhanced bandwidth [10, 46] with some trade-off with the gain.

The performance of antenna is studied by observing field patterns that are obtained by solving Maxwell equations numerically. Though the values of field components become known, it remains difficult to get the physical insight of the operation mechanism in complex structures. This is greatly facilitated by developing an equivalent circuit model of the antenna system by involving lumped elements. A resonator, in general, may be represented by a

Table 2 Variation of bandwidth and gain in RDRA arrangements with dielectric loss

Design arrangements	Dielectric loss	Band width (GHz)	Maximum gain	Shape
1. Single RDRA	0.0	0.14	5.53	Apple
	0.001	0.14	5.26	Apple
	0.01	0.14	4.82	Deformed
	0.1	–	− 4.48	Deformed
2. Array of two RDRA's	0.0	0.97	5.20	Apple
	0.001	0.97	4.97	Apple
	0.01	0.92	3.18	Apple
	0.1	1.04	2.90	Deformed
3. Array of three RDRA's (all aperture coupled)	0.0	1.34	2.55	Deformed
	0.001	1.35	2.34	Deformed
	0.01	1.37	1.84	Deformed
	0.1	1.4	1.58	Deformed
4. Array of three RDRA's (middle parasitic)	0.0	1.32	5.97	Apple
	0.001	1.33	5.69	Apple
	0.01	1.32	5.92	Apple
	0.1	1.36	5.81	Apple

circuit comprising of resistance (R_r), inductance (L_r) and capacitance (C_r) connected in a suitable way. For example, a resonator made of a piezoelectric ceramic such as PZT may be represented by an equivalent circuit comprising of a series combination of resistance (R_r), inductance (L_r) and capacitance (C_{r1}), further connected in parallel to a capacitor C_{r2} [14, 47, 48]. Expressions for obtaining the values of such lumped components for resonators working at microwave frequencies are available in the literature [49, 50]. The values of the lumped components used in the equivalent circuit model are obtained by comparing the behaviour predicted by the model with that obtained from numerical simulations. The antenna performance can be visualized by varying the values of components. An equivalent circuit model for microstrip aperture-coupled RDRA is shown in Fig. 4 where $M1$ and M denote the inter-segment coupling and subscripts 'm' and 'slot' denote the quantities related to the microstrip and slot, respectively. Expressions for the lumped component are given below in Eqs. (12–14) [50, 51].

$$R_r = \frac{2n^2 Z_0 S_{11}}{S_{11}} \tag{12}$$

$$C_r = \frac{Q_0}{\omega_0 R_r} \tag{13}$$

$$L_r = \frac{1}{C_r \omega_0} \tag{14}$$

Here, the subscript r denotes the quantities related to the DRA, S_{11} is the reflection coefficient, Z_0 the characteristic impedance, Q_0 the quality factor, n is the coupling magnitude between dielectric resonator and excitation source and ω_0 the angular frequency. The values of the lumped components used in the equivalent circuit model are obtained by comparing the behaviour predicted by the model with that obtained from numerical simulations.

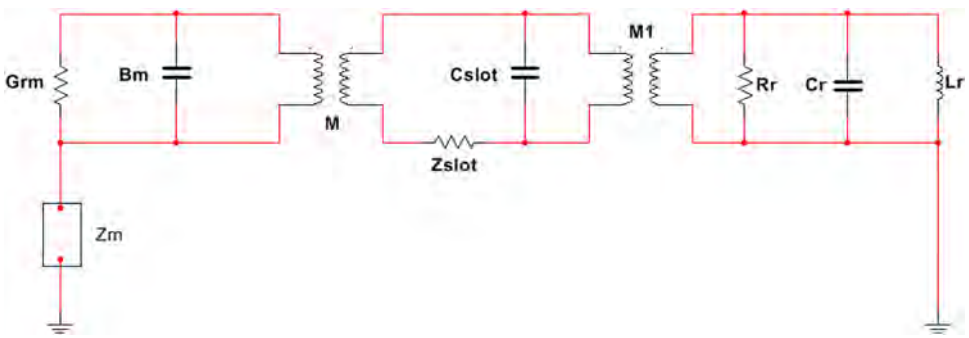

Fig. 4 Equivalent circuit of microstrip slot-coupled RDRA

3 Conclusions

The basics of design of microstrip aperture-coupled ceramic rectangular dielectric resonator antenna (RDRA), which include estimation of RDRA dimensions and microstrip width depending on the value of relative dielectric permittivity (ε_r) and operating/resonant frequency, have been described. The RDRA dimensions were calculated by solving the transcendental equation derived from Maxwell equations using dielectric waveguide model (DWM). Some ceramics found useful for fabrication of DRAs have been presented. To explore possible application of ceramics having small dielectric loss (tan $\delta \sim 0.1$), RDRA arrays comprising of configurations using one, two and three elements (with $\varepsilon_r = 40$) were designed, and effect of dielectric loss on the performance was studied using ANSYS HFSS simulations. It was found that for array comprising of three elements, when the outer elements were aperture coupled and the middle parasitic element had small dielectric loss (tan $\delta \sim 0.1$), the bandwidth got enhanced by 3% and the gain decreased only by 2.7% with the far field pattern remaining almost same. This indicated that ceramics with small dielectric loss such as $Ba_{1-x}Sr_xTiO_3$ ($x = 0.35$, tan $\delta \sim 0.1$) could be used for development of RDRA with some trade-off with gain by using suitable designs. Equivalent circuit modelling useful in development of rectangular DRA was also described.

Acknowledgements The financial support received by one of the authors (SP) from IIT(BHU) in the form of Teaching Assistantship is gratefully acknowledged.

References

1. Huang Y, and Boyl K, *Antennas from Theory to Practice*, Wiley, New York (2008), p 3.
2. Schelkunoff S A, and Friis H T, *Antennas Theory and Practice*, Wiley, New York (1952).
3. Kraus J D, *Antennas*, McGraw-Hill Book Co, New York (1988).
4. Keyrouz S, Caratelli D, and Favreau D, *Dielectric Resonator Antennas for 5G Applications*, http://www.mpdigest.com/2017/04/24/dielectric-resonator-antennas-for-5g-applications/, Accessed on 15 Aug 2018.
5. Keyrouz S, and Caratelli D, *Int J Antennas Propag* **2016** (2016) 1.
6. Richtmyer R D, *J Appl Phys* **10** (1939) 391.
7. Long S A, McAllister M A, and Shen L C, *IEEE Trans Antenna Propag* **AP-31** (1983) 406.
8. Yaduvanshi R S, and Parathasarathy H, *Rectangular Dielectric Resonator Antennas*, Springer, New Delhi (2016).
9. Min K, and Tran V, *J Korean Electromagn Soc* **6** (2006) 165.
10. Zivkovic I, *Progr Electromagn Res C* **30** (2012) 241.
11. Huitema L, and Monediere T, in *Dielectric Material*, (ed) Silaghi M A, IntechOpen (2012); https://doi.org/10.5772/50612. Available from: https://www.intechopen.com/books/dielectric-material/dielectric-materials-for-compact-dielectric-resonator-antenna-applications.
12. Sadiku M N O, *Principles of Electromagnetics*, 4th ed., Oxford University Press, New Delhi (2007).
13. Kraus J D, and Carver K R, *Electromagnetics,* McGraw-Hill, Tokyo (1980).
14. Moulson A J, and Herbert J M, *Electroceramics*, Wiley, Chichester (2003).
15. Gevorgian S, *Ferroelectrics in Microwave Devices, Circuits and Systems*, Springer, London (2009).
16. Sengupta L C, and Sengupta S, *IEEE Trans Ultrason Ferroelectr Freq Control* **44** (1997) 792.
17. Konishi Y, *Proc IEEE* **79** (1991) 726.
18. Sulong T A T, Osman R A M, and Idris M S, in *AIP Conf Proc The 2nd International Conference on Functional Materials and Metallurgy (ICoFM 2016) AIP Conf Proc*, Vol 1756, pp 070003-1–070003-7; https://doi.org/10.1063/1.4958779. Published by AIP Publishing. 978-0-7354-1414-3.
19. Vopson M M, *Crit Rev Solid State Mater Sci* **40** (2014) 1.
20. Fiebig M, Lottermoser T, Meier D, and Trassin M, *Nat Rev Mater* **1** (2016) 1.
21. Sengupta L C, and Sengupta S, *Mater Res Innovat* **2** (1999) 278.
22. Mosallaei H, and Sarabandi K, *IEEE Trans Antennas Propag* **52** (2004) 1558.
23. Rocha H H B, Frere F N A, Santos M R P, Sasaki J M, Cordaro T, and Sombra A S B, *Physica B* **403** (2008) 2902.
24. Su H, Tang X, Zhang H, Jing Y, *J Electron Mater* **43** (2014) 299.
25. Petosa A, and Ittipiboon A, *IEEE Antennas Propag Mag* **52** (2010) 91.
26. Mongia R K, and Bhartia P, *Int J Microw Millim Wave Comput Aided Eng* **4** (1994) 230.
27. Petosa A, Ittipiboon A, Antar Y, in *Dielectric Resonator Antennas*, (eds) Luk K M, and Leung K W, Research Studies Press Ltd., Baldock (2003).
28. Mongia R K, and Ittipiboon A, *IEEE Trans Antennas Propag* **45** (1997) 1348.
29. Okaya A, and Barash L F, *Proc IRE* **50** (1962) 2081.
30. Sebastian M T, *Dielectric Materials for Wireless Communications*, Elsevier Ltd., Oxford (2008).
31. Sebastian M T, Silva M A S, and Sombra A S B, in *Microwave Materials and Applications*, Vol I, (eds) Sebastian M T, Ubic R, and Jantunen H, Wiley, London (2017), p 1.
32. Sebastian M T and Jantunen H, *Int Mater Rev* **53** (2008) 57.
33. Sebastian M T, Ubic R and Jantunen H, *Int Mater Rev* **60** (2015) 392.
34. Lee D Y, Yoon S J and Yeo J H, *J Mater Sci Lett* **19** (2000)131.
35. Seabra M P and Ferreira V M, *Mater Res Bull* **37**(2002) 255.
36. Lin H, Luo L, and Chen W, *Mater Lett* **62** (2008) 611.
37. Gangwar R K, Singh S P, Choudhary M, Kumar D, Rao G L N, and Raju K C J, *J Ceram* **2013** (2013) 1.
38. Peng Z, Wang H, and Yao X, *Ceram Int* **30** (2004) 1211.
39. Gangwar R K, Singh S P, and Kumar D, *Prog Electromagn Res B* **31** (2011) 157.
40. O'Reilly T P A, Ruytenberg T, and Webb A G, *Magn Reson Med* **79** (2018) 1781.
41. de Medeiros J L G, de Araujo W C, d'Assuncao A G, de Mendonca L M, and de Oliveira J B L, *Microw Opt Technol Lett* **55** (2013) 1352.
42. Ene-Dobre M, Banciu M G, Nedelcu L, Ioachim A, and Alexandru H V, *J Optoelectron Adv Mater* **12** (2010) 1926.
43. Kumari P, Tripathi P, Sahu B, Singh S P and Kumar D, *J Electron Mater* **47** (2018) 5218.
44. Gangwar R K, Singh S P, Choudhary M, Singh N K, Kumar D, Rao G L N, and Raju K C J, *J Alloys Compd* **509** (2011) 10195.
45. Tripathi P, Sahu B, Kumari P, Parkash O, Singh S P, and Kumar D in *2015 IEEE Applied Electromagnetics Conference (AEMC), Guwahati* (2015), p 1.
46. Lee J P Y, and Balmain K G, *Radio Sci* **14** (1979) 437.

47. Chaitanya P, Shukla A, and Pandey L, in *The 15th International Conference of International Acad of Physical Sciences* Dec 9–13 2012, Pathumthani, Thailand, pp 73–79.
48. Chaitanya P, Shukla A, and Pandey L, *Integr Ferroelectr Int J* **150** (2014) 88.
49. Collin R E, *Foundations for Microwave Engineering*, 2nd ed., Wiley, Hoboken (2001), p 514.
50. Ain M F, Qasaymeh Y M, Ahmad Z A, Zakariya M A, and Ullah U, in *Proc Progress in Electromagnetic Research Symposium, KL, Malaysia* (2012), p 1837.
51. Baba A A, Zakariya M A, Baharudin Z, Rehman M Z U, Ain M F, and Ahmad Z A, *Prog Electromagn Res C* **45** (2013) 15.